Available online at www.sciencedirect.com
ScienceDirect
Energy Reports 9 (2023) 172–183
www.elsevier.com/locate/egyr

TMREES23-Fr, EURACA 06–08 February 2023, Metz-Grand Est, France

Reliability of autonomous solar-wind microgrids with battery energy storage system applied in the residential sector

Eliseo Zarate-Perez[a,b,*], Cesar Santos-Mejía[a], Rafael Sebastián[a]

[a] *Escuela Internacional de Doctorado (EIDUNED), Universidad Nacional de Educación a Distancia (UNED), C/Bravo Murillo, 38, Madrid, 28015, Spain*
[b] *Department of Engineering, Universidad Privada del Norte (UPN), Av. Alfredo Mendiola 6062, Los Olivos 15314, Peru*

Received 17 May 2023; accepted 26 May 2023
Available online 8 June 2023

Abstract

Residential electricity generation can benefit from the successful deployment of photovoltaic (PV) and wind renewable energy sources. However, their intermittent nature poses a significant limitation. To address this, a hybrid system can be employed to enhance system reliability and efficiency. Reliability analysis plays a crucial role in evaluating the energy production capacity to meet the demand. This study aims to assess the reliability of a hybrid PV/wind microgrid through simulation. Data from a residence were collected every 10 s, and average values were computed on an hourly basis and exported for computer processing. Solar irradiation, wind speed, and temperature data were also utilized. The modeling process involved defining the PV panel, wind turbines, battery energy storage system (BESS), management strategy, and energy autonomy. The results indicate that when PV and wind systems operate independently, they are unable to consistently reduce the residential energy deficit. However, the PV/Wind/BESS configuration significantly improves system operation and proves sufficient to meet the required load in most hours. Through this configuration, only 42.5% of the total PV/wind energy utilized by the residents needs to be dispatched through the BESS. Moreover, the BESS capacity is reduced by 50% when the systems are used separately. The public grid only supplies power when the BESS is insufficient to cover the load. Therefore, the optimal sizing of the BESS plays a critical role in system viability, reducing initial installation costs, regulating microgrid parameters, and contributing to the reduction of the energy deficit. Hence, investigating the fundamental design parameters of the microgrid and BESS is essential for identifying the optimal capacity of the system and ensuring model reliability.

Peer-review under responsibility of the scientific committee of the TMREES23-Fr, EURACA, 2023.

Keywords: Autonomous solar-wind microgrids; Hybrid pv/wind microgrid; Reliability analysis; Renewable energies; Energy deficit

1. Introduction

Renewable energy sources are omnipresent in the construction of a pollution-free world. Therefore, photovoltaic (PV) and wind-renewable sources can be successfully implemented to generate residential electricity [1], supporting

* Corresponding author at: Escuela Internacional de Doctorado (EIDUNED), Universidad Nacional de Educación a Distancia (UNED), C/Bravo Murillo, 38, Madrid, 28015, Spain.

E-mail addresses: ezarate9@alumno.uned.es, eliseo.zarate@upn.edu.pe (E. Zarate-Perez).

https://doi.org/10.1016/j.egyr.2023.05.239

Peer-review under responsibility of the scientific committee of the TMREES23-Fr, EURACA, 2023.

Nomenclature

A_{PV}	Area of the PV panel
BESS	Battery energy storage system
BTM	Behind the Meter
DNI	Direct normal irradiance
GHI	Global horizontal irradiance
IEC	International electrotechnical commission
NOCT	Nominal operating temperature of the PV cells
NSRDB	National Solar Radiation Database
PV	Photovoltaic
T_a	Ambient temperature
TED	Total Energy Deficit
Y_d	Reduction factor for dust accumulation
η_{PV}	Conversion efficiency of PV panel

a sustainable solution to the global energy crisis [2]. In particular, energy consumption in the residential sector represents 30% of global energy demand. This is expected to increase owing to economic growth, urbanization, improved quality of life, and globalization [3]. Therefore, using renewable energy in the domestic and residential sectors play an imperative role in achieving a sustainable development agenda. However, the major limitation of renewable-energy networks is their intermittent nature. Therefore, using a hybrid system with two or more renewable sources could reduce this limitation by offering increased system reliability and efficiency [4].

The concept of reliability is related to the systematic and rigorous analysis of functional problems in renewable energy generators. This analysis was conducted to determine the design of a reliable energy system. Reliability is an engineering specialty that analyzes and evaluates the ability of energy production to meet the energy demands [5]. Thus, upcoming technological solutions for hybrid renewable energy systems are expected to experience high levels of reliability and efficiency. These systems are fundamental for the following reasons: they are available in nature, friendly to the planet, and are considered appropriate and beneficial energy sources due to their availability and topological advantages for energy generation [6]. Some studies have demonstrated that hybrid microgrids can improve system reliability and provide a cost-effective power supply than single-power microgrids [7].

However, determining the optimal installation capacity of microgrids is considered an essential problem to ensure the efficient use of generation sources in hybrid systems [8,9]. The optimal installation capacity of a hybrid system, in turn, can meet a consumer's reliable demand for energy. Thus, an installation that is overpowered or oversized could lead to high installation and energy production costs. The installation of a system with power below the required level compromises the reliability of the electrical supply [10]. Various methodologies have been presented to approach the optimal capacity and difficulty of hybrid microgrids for different purposes and functionalities [11,12]. Occasionally, the topology of hybrid microgrids allows a sufficient balance between renewable energy generation and residential energy requirements. However, renewable energy systems need to perform a reliability analysis to determine the energy deficit, thus ensuring the optimal capacity of the system.

Consequently, most studies conducted to determine the dimensioning of the microgrid have considered complementary design criteria. These include techno-economic feasibility [13], life cycle costs [14], levelized energy costs [15], indicators of environmental impacts [16], mathematical approaches, or using software, such as HOMER [17]. However, several reported studies assume load consumption by implementing a normalized standard profile, assuming a nominal power demand, and considering a randomness factor to introduce variability. Due to the intermittent, random, and seasonal nature of renewable resources, autonomous microgrids based on the analysis of these characteristics of the demand profile pose a severe threat to the reliability of the system.

Real data on residential energy demand are required to understand the intermittent behavior of renewable resources in response to energy demand. Short-term solar radiation variability is a key feature for understanding solar resources and the dynamic characteristics of renewable energy production, with significant transient effects on microgrid performance [18]. Therefore, understanding the dynamics of resources and how they affect energy production is essential for the proper management of solar resources in response to residential demand. This study aimed to evaluate the reliability of a hybrid PV/wind microgrid by identifying the deficit and energy autonomy through a simulation. Similarly, a generalizable design methodology was presented to identify the installation power of the hybrid system based on reliability analysis using hourly data.

Consequently, considering the transient effects on the performance of microgrids, such as the variability of short-term solar radiation, the dynamic characteristics of PV/wind energy production against residential demand should be identified. Similarly, the BESS can contribute to sufficient flow of renewable energy to cover the required residential load. However, a significant reduction in the installed power of the BESS I s expected because of the reduction in the production variability of the hybrid PV/wind system. The optimal dimensioning of the BESS in a microgrid can influence the viability of the system by reducing the initial installation costs.

2. System description and modeling

The evaluated system was a microgrid (Behind the Meter—BTM) comprising solar, wind, and battery energy storage system (BESS) generation sources. To summarize, the network topology is assumed to be a single AC bus where the loads are bundled and connected, as shown schematically in Fig. 1. Table 1 shows the details and basic parameters of the solar panel, inverter, BESS, and wind turbine. These parameters were used in the simulation analysis because they were commercial devices that were readily available in the local market. This section describes the databases used, solar PV and wind energy production systems, BESS, management strategies, and energy autonomy.

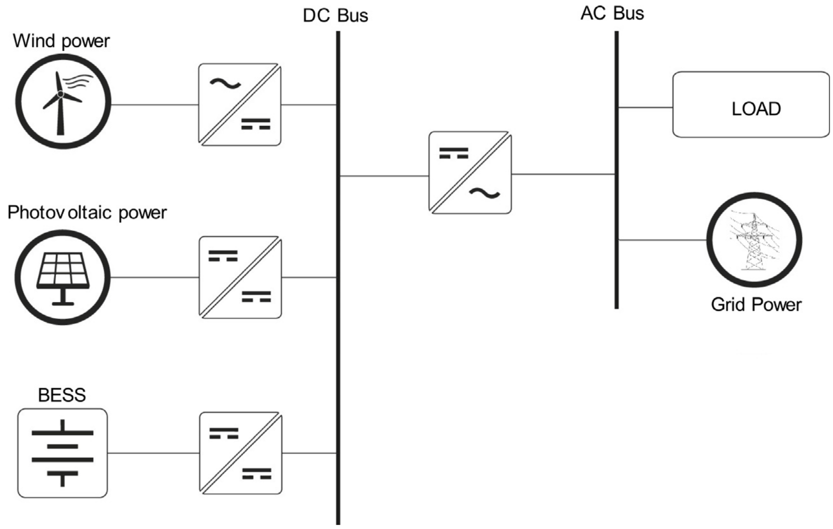

Fig. 1. Topology of the photovoltaic (PV)/Wind generation system with battery energy storage system (BESS).

Table 1. Basic parameters of the solar panel, inverter, battery energy storage system (BESS), and wind turbine.

250 W solar panel	Hybrid solar inverter	BESS	Wind turbine
Power max (Pm): 250 W Short circuit current (Isc): 8.95 A Maximum voltage (Vmp): 29.95 V Open circuit voltage (Voc): 37.25 V Efficiency: 19.9% Max power current (Imp): 8.35 A	Max. output power: 3000 W Inverter efficiency: 99.5% PV volt. Range: (150–550) V Output current: 16–27 A Input voltage: 150–550 V Nominal AC output: 230 V Number of MPP trackers: 2	Nominal voltage: 48 V Nominal capacity: 2400 Wh Usable capacity: 2280 Wh Charge voltage: 52.5–53.5 V Discharge Vol.: (44.5–53.5) V Charge/discharge current: 25 A (Recommend), 50 (Max), 90 (Peak@15s)	Rated power: 1000 W Maximum power: 1300 W Start-up wind speed: 2.5 m/s Rated wind speed: 10 m/s Rated voltage: 48 V Wheel diameter: 2.5 m Number of blades: 3

2.1. Databases collected

In this study, data were collected from the demand for electrical energy in a typical house located in the city of Lima, Peru. The data collected from the home meter were captured every 10 s with 1-h averages and exported for processing on a computer. Fig. 2 displays the hourly frequency of residential energy demand data for a full year. Similarly, data on solar irradiation, wind speed, and temperature downloaded from the National Solar Radiation Database (NSRDB) [19] were used. The NSRDB irradiance data was validated, revealing a correlation with surface observations and exhibiting mean percentage biases of less than 5% for global horizontal irradiance and less than 10% for direct normal irradiance [20].

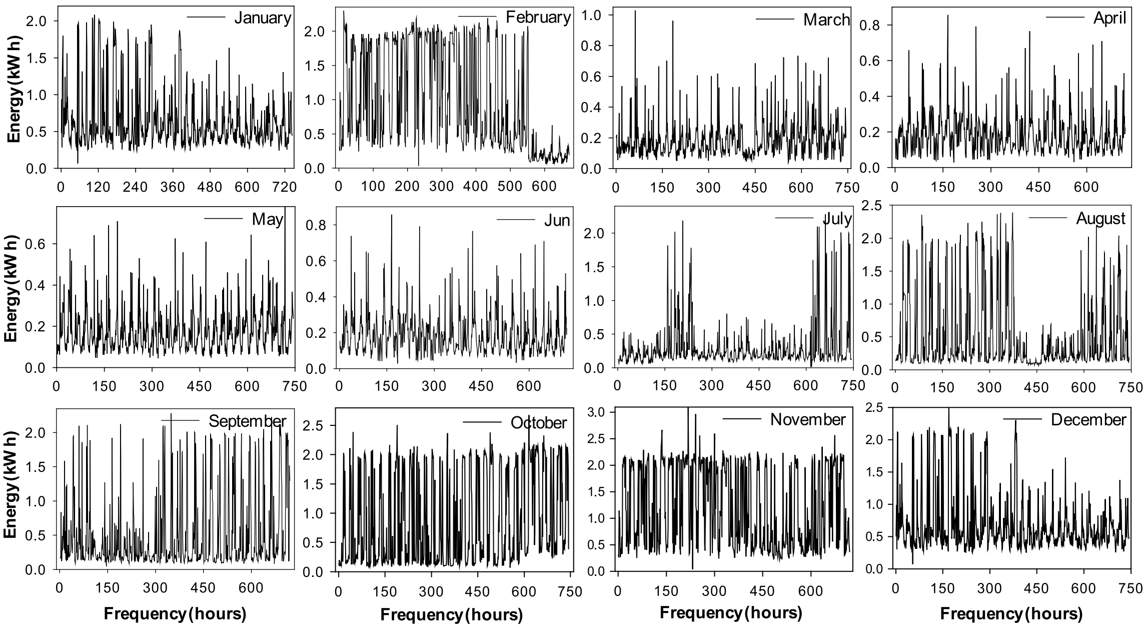

Fig. 2. Residential energy demand data.

2.2. Modeling of the PV panel

The input variables used for the PV panel model were solar irradiation (I) and ambient temperature (T_a), obtained from the NSRDB. Initially, the cell temperature was calculated using Eq. (1) [4,21].

$$T_C(t) = T_a(t) + I(t)\left(\frac{NOCT - 20}{0.8}\right), \tag{1}$$

where NOCT is the nominal operating temperature of the PV cells. Using the results of Eq. (1), the output power of a PV panel was calculated according to Eq. (2) [22].

$$P_{PV\,unit}(t) = (Y_d)(\eta_{PV})(A_{PV})(I(t))\left(1 - \frac{K_p}{100\,(T_C(t) - 25)}\right), \tag{2}$$

where Y_d represents the reduction factor for dust accumulation, η_{PV} stands for the conversion efficiency of the PV panel, A_{PV} indicates the area of the PV panel, and Kp denotes the temperature coefficient. Therefore, the Eq. (3) defines the total power generated ($P_{PV}(t)$) by a set of panels [23].

$$P_{PV}(t) = (N_{PV})(P_{PV\,unit}(t)) \tag{3}$$

2.3. Modeling of the wind turbines

In order to conduct the modeling, the variation in wind speed with height was taken into account. Hence, the Eq. (4) describes the relationship between the wind speed measured at the anemometer height and the desired height of the wind turbine hub [24].

$$\frac{v_2}{v_1} = \left(\frac{h_2}{h_1}\right)^{\alpha}, \tag{4}$$

where v_1 and v_2 represent the speeds at reference height h_1 and hub height h_2, respectively, while α denotes the coefficient of friction. The coefficient of friction encompasses various factors such as the roughness of the terrain, wind speed, temperature, height above the ground, time of day, and time of year [25]. Different terrain characteristics are associated with the coefficient of friction according to the technical literature [26]. However, the IEC standards [24] suggest a friction coefficient value of 0.11 for extreme wind conditions and 0.20 for normal wind conditions. The power output of a wind turbine can be determined using Eq. (5) [6]:

$$P_{(WTunit)}(t) = \begin{cases} 0;\ V(t) < V_{cut-in} \\ \dfrac{P_{WTr}\left(V^3 - V_{cut-in}^3\right)}{(V_{rated}^3 - V_{cut-in}^3)};\ V_{cut-in} \leq V(t) < V_{rated} \\ P_{WT} \quad ;\ V_{rated} \leq V(t) < V_{cut-out} \\ 0;\ V_{cut-out} \leq V(t) \end{cases}, \tag{5}$$

The output power of a wind turbine, represented as $P_{(Wtunit)}$, depends on two key factors: the rated power of the turbine, P_{WTr}, and the wind speed, V. In addition, there are several essential wind speed values used to regulate the turbine's operation. V_{cut-in} denotes the minimum wind speed required to initiate the turbine's operation, V_{rated} indicates the wind speed at which the turbine operates at its maximum rated power, and $V_{cut-out}$ represents the wind speed at which the turbine is safely shut down. These wind speed values play a critical role in ensuring the turbine operates efficiently and within its designated parameters, prioritizing both performance and safety. The total power ($P_{WT}(t)$) generated by a set of wind turbines is determined using Equation (6) [4].

$$P_{WT}(t) = (N_{WT})(P_{WTunit}(t)) \tag{6}$$

2.4. BESS

Eq. (7) offers a dependable approach for calculating the charging process of the Battery Energy Storage System (BESS), considering the energy balance between the production units and the residential energy demand. Likewise, Eq. (8) is utilized to enable the discharge process [6] area of the PV panel, and Kp denotes the temperature coefficient [6].

$$E_{bat}(t) = E_{bat}(t-1)(1-\sigma) + \left[E_{gen}(t) - \frac{E_{required}(t)}{\eta_{inv}}\right]\eta_B, \tag{7}$$

$$E_{bat}(t) = E_{bat}(t-1)(1-\sigma) + \left[(\frac{E_{required}(t)}{\eta_{inv}}) - E_{gen}(t)\right]\eta_B, \tag{8}$$

In the given equation, various variables are defined. $E_{Bat}(t)$ represents the energy stored in the BESS at hour t, measured in watt-hours (Wh). $E_{Bat}(t-1)$ represents the energy stored in the BESS at the previous hour (t – 1) in watt-hours (Wh). σ represents the self-discharge rate per hour. For lithium–iron–phosphate batteries, the typical self-discharge rate is approximately 0.3% [27]. $E_{Required}(t)$ represents the hourly energy demand from the residential load, as illustrated in Fig. 1. η_{inv} signifies the efficiency of the inverter, as outlined in Table 1, whereas η_B denotes the efficiency of the BESS, also mentioned in Table 1. Additionally, $E_{Gen}(t)$ symbolizes the energy generated by the PV/wind system at each specific hour (t). Thus, $E_{Gen}(t)$ is given by Eq. (9) [6].

$$E_{Gen}(t) = (N_{PV})(E_{PV}(t)) + (N_W)(E_W(t)), \tag{9}$$

where $E_{PV}(t)$ represents the hourly energy produced by the PV module, while $E_W(t)$ signifies the energy generated by the wind turbine. The variables N_{PV} and N_W refer to the respective quantities of PV modules and wind turbines. The charge level of the battery bank must adhere to the constraint expressed in Eq. (10) at any given time (t) [6].

$$E_{Bat,min} \leq (E_{Bat}(t)) \leq (E_{Bat,max}) \tag{10}$$

The maximum energy stored in the BESS, referred to as $E_{Bat,max}$, is equivalent to the nominal capacity (NC) of the battery bank. Similarly, the minimum capacity of the BESS, denoted as $E_{Bat,min}$, is determined by taking into account the maximum depth of discharge (DoD), as demonstrated in Eq. (11). Based on the technical characteristics, the optimal utilization of lithium–iron–phosphate batteries for enhancing their useful life is achieved when the depth of discharge (DoD) is limited to 80% [27].

$$E_{Bat,min} = (1 - DoD)(CB) \tag{11}$$

2.5. Management strategy and energy autonomy

We propose a hybrid system management strategy that utilizes residential energy demand as a basis. The strategy operates as follows:

(a) If the energy generated from PV/wind sources exceeds the energy required by the residence, the surplus energy is stored in the BESS. The state of charge of the BESS is then calculated using Eq. (7).

(b) When the energy demand surpasses the generated energy, the BESS is utilized to meet the load demand. In such cases, the new state of charge of the BESS at hour (t) is updated using Eq. (8).

(c) In the event that the state of charge of the BESS reaches its minimum level ($E_{Bat,min}$), any energy deficit is covered by the public energy network. This approach reduces the reliance on energy injections from the public grid, while also posing a challenge in limiting the BESS load to PV/wind energy.

By establishing the optimal energy autonomy of a hybrid PV/wind system based on residential energy demand, we can achieve a reliable and cost-effective energy supply [6]. The system's reliability can be evaluated through the Total Energy Deficit (TED), which represents the proportion of renewable energy that is not provided to the consumer when requested, relative to the total energy demand. This relationship is expressed in Eq. (12) [6].

$$TED = \left(\sum_{t=1}^{T} \frac{E_{required}(t) - E_{Supp}(t)}{E_{required}(t)}\right), \tag{12}$$

where $E_{Required}(t)$ is the energy demanded by the consumer in hour t, and T represents the total data analyzed (one year). Similarly, $E_{Supp}(t)$ is the energy per hour supplied to the consumer from the production of the hybrid PV/wind system and the current state of the BESS at hour (t) according to Equation (13) [4]. Consequently, if there is an energy deficit at any hour t, the deficit is covered by the supply from the public grid.

$$E_{Supp}(t) = \left[E_{Gen}(t) + E_{Batt}(t-1) - E_{Batt,min}\right]\eta_{Inv} \tag{13}$$

Lastly, from the TED, energy autonomy $E_{Autonomy}(t)$ can be expressed as a percentage of the hybrid PV/wind system. Thus, energy autonomy is the ability of the PV/wind system to meet the energy needs of a residence without relying on energy from the public grid, as shown in Eq. (14) [4].

$$E_{Autonomy}(t) = (1 - TED) * 100\% \tag{14}$$

A program was developed to validate the model using the widely-used free software R Core Team [28], which is renowned for its effectiveness in time-series modeling and process optimization, among other applications.

3. Simulation results and discussions

This section presents simulation results that analyze the impact of the production of a hybrid PV/wind system in response to residential demand to assess energy autonomy. Therefore, the energy balance of the microgrid per hour was calculated considering the generated and consumed power, storage capacity, and dispatch strategies. Based on this, the reliability criteria and degree of autonomy of the hybrid microgrid were calculated.

Fig. 3(a) shows the results of energy autonomy from the November 8–11, with a capacity of 1.5 kWp for the installation power of the PV system and 1.0 kWp for the installation of the wind turbine. The results indicate that the PV/wind microgrid only achieves an autonomy of 75%, 30%, 23%, and 75% for 21–24 h on November 8, respectively. Similarly, Fig. 3(b) shows the energy balance, where $E_{gen,use}(t)$ comprises the PV/wind energy that is directly consumed without passing through the BESS.

Additionally, the energy supplied by the BESS is shown when there is an energy deficit caused by the hybrid microgrid in response to the demand. Finally, the equivalent energy deficit assumed by the energy of the public grid is shown. This figure strongly suggests that the sum of the three components is equivalent to the energy required ($E_{Required}$ (t)) by the residence.

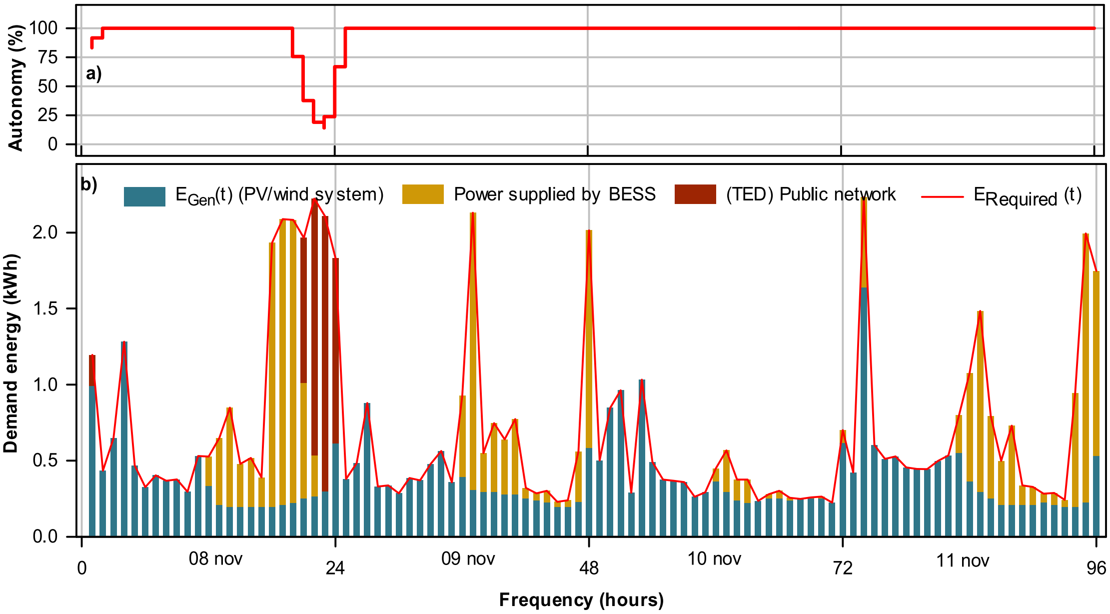

Fig. 3. (a) Energy autonomy for November 08–11. (b) Energy balance for the same period.

Fig. 4 shows the microgrid performance with only the PV generation considering different PV installation capacities. We found that for an installation power of 1 kWp for the PV generation system, acceptable autonomy is achieved for the months of March, April, and May. For a 2 kW installation, energy efficiency improved from March to July. In addition, the scenario is further improved for a PV system with a capacity of 3 kWp. Although the installed capacity of the system increased by 4 kWp, there was no consistent difference. As a result, this is not necessarily related to the power capacity of the BESS. This is rather related to energy demand versus available solar resources and their stationary characteristics. This is consistent with other studies. These studies report that solar energy systems located in several countries of the Andes do not achieve energy autonomy with a TED of 0% [29].

Thus, the peak hours of data collected from the energy demand were identified to determine the capacity of the BESS. Consequently, a lithium–iron–phosphate BESS with a capacity of 4.8 kWh was chosen, which was sufficient to deliver energy under the established conditions of peak hour periods. Similarly, lithium-ion iron phosphate technology has a relatively high discharge cycle number, which is approximately 6000 or more when the DoD is set to 80%. Furthermore, the cycle efficiency was 85% for the AC-coupled version [30]. Thus, the BESS could last for more than 16 years, taking these factors into account.

Fig. 5 illustrates the autonomy of the microgrid when only wind energy is considered. The microgrid with a turbine capacity of 1 kWp presented an energy deficit for most months of the evaluation period. Evidently, the panorama of autonomy improves with an increase in installation power from 1.5 kWp to 2.5 kWp; however, this autonomy does not fully cover the months of January, February, November, and December. According to the literature, there are several applications for individual systems, both for generation and energy storage. However, these approaches have limitations in their ability to adapt to the seasonal characteristics of the energy demand. In contrast, hybrid microgrids exhibit increased flexibility in response to consumer energy demand, as shown in Fig. 6. Considering that energy production is based on highly intermittent solar radiation and wind speed, the results indicate considerable potential for minimizing energy loss.

The PV/Wind/BESS configuration significantly enhances performance during daylight hours, as illustrated in Fig. 6. The combined output power of the PV panels and the wind turbine proves adequate to meet the required load for the majority of hours. Moreover, any excess PV/wind energy is directed towards the BESS in case of an energy deficit. Consequently, energy from the public grid is only injected when the BESS is unable to fulfill the load requirements. As a result, the public power system typically serves as a backup power source during nighttime and off-peak hours.

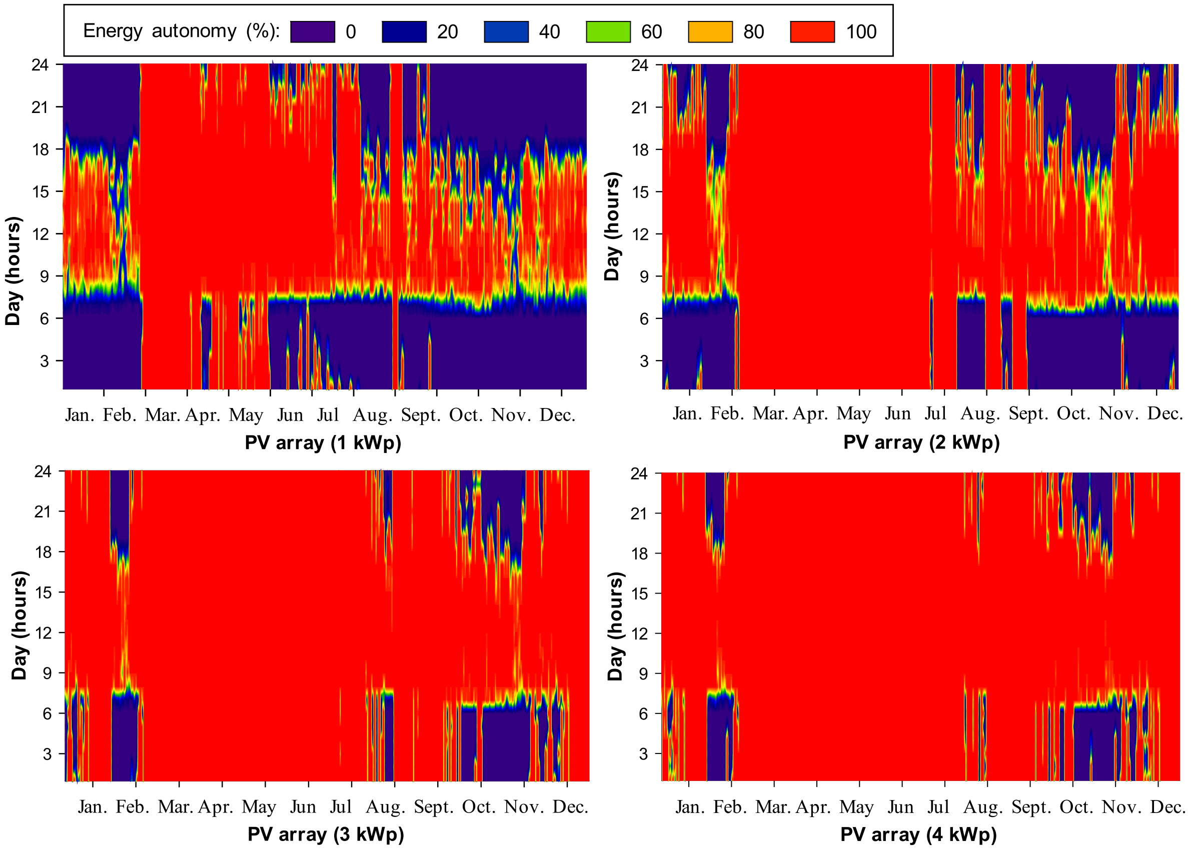

Fig. 4. Energy autonomy considering only the photovoltaic solar microgrid.

For a PV system with an installation power of 1 kWp plus a 1 kWp wind turbine and a BESS of 4.8 kWh, an energy deficit is evident. This is because high renewable energy production is required. Similarly, for 2 kWp of PV system power and 1 kWp of wind turbine power, the autonomy of the microgrid increases. However, this is due to an energy deficit in January, February, October, November, and December. With PV power of 2.5 kWp and wind power of 1 kWp, the energy deficit is reduced, improving the degree of autonomy steadily. Nevertheless, the BESS capacity of 4.8 kWh has remained constant. However, considering that the PV/wind energy injected directly into the power load of the residence comprises more than 50% of the total renewable energy, the optimal dimension of the BESS is 2.4 kWh. This significantly reduces the capacity of the BESS, thus increasing the viability of the microgrid. Therefore, the optimal dimension of the hybrid system of the microgrid is 2.4 kWp for the PV system and 1.5 kWp for the wind turbine, as shown in Fig. 6(d).

In this study, only 42.5% of the total PV/wind energy used by the residence was dispatched through BESS. Consequently, 57.5% was delivered directly to the housing load without passing through the BESS. According to Fig. 6, for a 2.5 kWp PV system array, 1.5 kWp of wind turbine power, and a BESS of 2.4 kWh capacity, the hybrid microgrid's autonomy slightly improved in comparison to a 2.5 kWp PV system, 1.0 kWp of wind turbine power, and a 4.8 kWh BESS. Thus, the 50% reduction in the initially defined BESS capacity did not increase the energy deficit.

Several studies have focused on the optimal size of renewable energy generation systems and BESS. The techno-economic method has made it possible to identify the advantages of renewable systems compared with the application of the conventional grid [31]. In most cases, these approaches are limited because they fail to integrate real data on energy demand; instead, they are designed based on a normalized standard profile with nominal power demand and random factors to account for variability. The optimal dimensioning of BESS in a microgrid affects

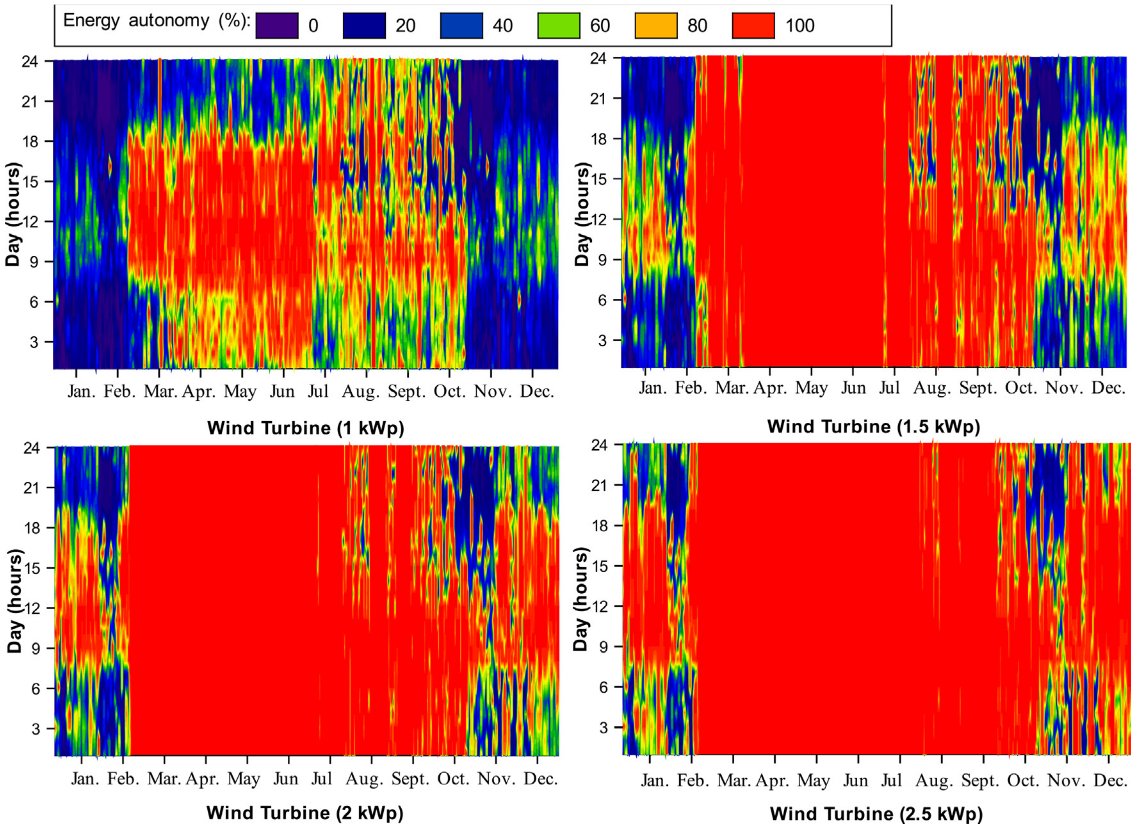

Fig. 5. Energy autonomy considering only the wind microgrid.

the viability of the system in several ways. This includes the initial installation costs, regulating the microgrid parameters, and contributing to the reduction of the energy deficit in the system.

Thus, the basic design parameters of the microgrid and BESS must be considered to determine the optimal system capacity for the model to be reliable. Consequently, it is recommended that real data or realistic projections along with frequent time series be used to obtain optimal results for improved sizing. Short-term solar radiation variability is considered a key feature in identifying a better understanding of the dynamic characteristics of PV/wind power production, with significant transient effects on microgrid performance. Therefore, identifying energy dynamics and determining how they affect energy production are essential in response to residential demand.

4. Conclusions

This study assessed the reliability of a hybrid PV/wind microgrid by identifying the deficit and energy autonomy through a simulation.

- The results indicate that both the PV/BESS and wind/BESS configurations are unable to mitigate the residential energy deficit when energy is generated independently.
- The PV/wind/BESS configuration enhances system operation and proves sufficient to meet the required load.
- In case of an energy deficit, any excess PV/wind energy can be utilized to supply power to the BESS.
- The public grid only injects energy when the BESS status is insufficient to cover the load.
- The public power system typically functions as a backup power source, operating primarily at night and during off-peak hours.
- Considering that PV/wind energy directly supplied to residential power load constitutes over 50% of the total renewable energy, this significantly reduces the power requirement of the BESS by 50%.

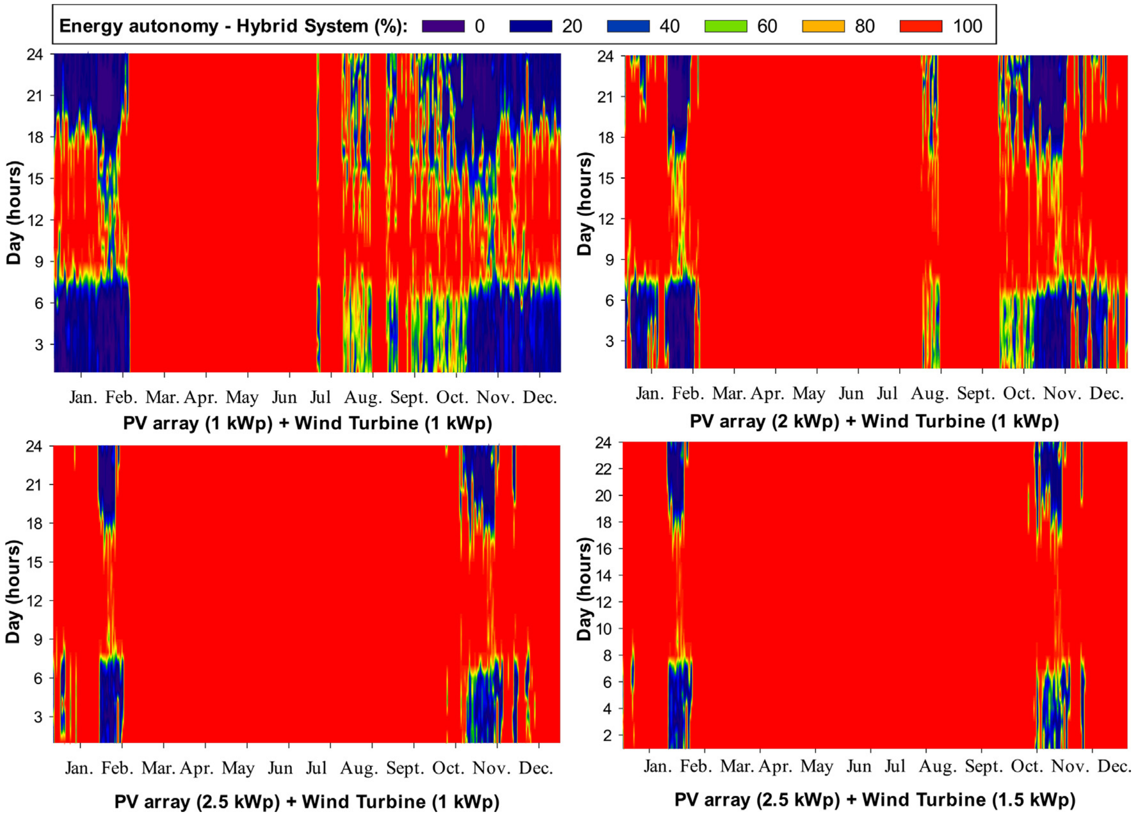

Fig. 6. Energy autonomy considering the photovoltaic (PV)/wind microgrid.

- The optimal sizing of the BESS in a microgrid plays a crucial role in the system's viability by minimizing initial installation costs, regulating microgrid parameters, and reducing the energy deficit.
- Determining the fundamental design parameters of the microgrid and BESS is necessary to identify the optimal capacity that ensures system reliability.
- It is generally recommended to incorporate real data or realistic load projections and utilize high-frequency time series (at least on an hourly basis) to achieve optimal results for improved sizing.

CRediT authorship contribution statement

Eliseo Zarate-Perez: Investigation, Formal analysis, Software, Writing – original draft, Writing – review & editing. **Cesar Santos-Mejía:** Conceptualization, Validation, Supervision, Writing – review & editing. **Rafael Sebastián:** Conceptualization, Validation, Supervision, Writing – review & editing.

Declaration of competing interest

The authors declare that they have no known competing financial interests or personal relationships that could have appeared to influence the work reported in this paper.

Data availability

The authors do not have permission to share data.

Funding

No specific grants were received from any funding agencies for this study.

References

[1] Fatin Ishraque M, Shezan SA, Ali MM, Rashid MM. Optimization of load dispatch strategies for an islanded microgrid connected with renewable energy sources. Appl Energy 2021;292:116879. http://dx.doi.org/10.1016/J.APENERGY.2021.116879.

[2] Zarate-Perez E, Rosales-Asensio E, González-Martínez A, de Simón-Martín M, Colmenar-Santos A. Battery energy storage performance in microgrids: A scientific mapping perspective. Energy Rep 2022;8:259–68. http://dx.doi.org/10.1016/J.EGYR.2022.06.116.

[3] Jakučionytė-Skodienė M, Dagiliūtė R, Liobikienė G. Do general pro-environmental behaviour, attitude, and knowledge contribute to energy savings and climate change mitigation in the residential sector? Energy 2020;193:116784. http://dx.doi.org/10.1016/J.ENERGY.2019.116784.

[4] Zarate-Perez E, Sebastián R. Autonomy evaluation model for a photovoltaic residential microgrid with a battery storage system. Energy Rep 2022;8:653–64. http://dx.doi.org/10.1016/J.EGYR.2022.07.085.

[5] Coit DW, Zio E. The evolution of system reliability optimization. Reliab Eng Syst Saf 2019;192:106259. http://dx.doi.org/10.1016/J.RESS.2018.09.008.

[6] Kaabeche A, Ibtiouen R. Techno-economic optimization of hybrid photovoltaic/wind/diesel/battery generation in a stand-alone power system. Sol Energy 2014;103:171–82. http://dx.doi.org/10.1016/J.SOLENER.2014.02.017.

[7] Neto PBL, Saavedra OR, Oliveira DQ. The effect of complementarity between solar, wind and tidal energy in isolated hybrid microgrids. Renew Energy 2020;147:339–55. http://dx.doi.org/10.1016/J.RENENE.2019.08.134.

[8] Chauhan A, Saini RP. A review on integrated renewable energy system based power generation for stand-alone applications: Configurations, storage options, sizing methodologies and control. Renew Sustain Energy Rev 2014;38:99–120. http://dx.doi.org/10.1016/J.RSER.2014.05.079.

[9] Grados J, Zarate-Perez E, Rubiños S, Meza J, Ortega-Rojas Y, Grados-Espinoza H, et al. Advance in wind energy systems: A bibliometric approach. In: Proc LACCEI int multi-conference eng educ technol 2022. 2022, http://dx.doi.org/10.18687/LACCEI2022.1.1.29.

[10] Upadhyay S, Sharma MP. A review on configurations, control and sizing methodologies of hybrid energy systems. Renew Sustain Energy Rev 2014;38:47–63. http://dx.doi.org/10.1016/J.RSER.2014.05.057.

[11] Lian J, Zhang Y, Ma C, Yang Y, Chaima E. A review on recent sizing methodologies of hybrid renewable energy systems. Energy Convers Manag 2019;199:112027. http://dx.doi.org/10.1016/J.ENCONMAN.2019.112027.

[12] Zarate-Perez E, Cornejo-Carbajal C, Grados J, Sebastián R. Energy autonomy in households using photovoltaic solar energy and battery energy storage: An evaluation model. In: Proc LACCEI int multi-conference eng educ technol 2022. 2022, http://dx.doi.org/10.18687/LACCEI2022.1.1.180.

[13] Mandal S, Das BK, Hoque N. Optimum sizing of a stand-alone hybrid energy system for rural electrification in Bangladesh. J Clean Prod 2018;200:12–27. http://dx.doi.org/10.1016/J.JCLEPRO.2018.07.257.

[14] Dufo-López R, Bernal-Agustín JL, Yusta-Loyo JM, Domínguez-Navarro JA, Ramírez-Rosado IJ, Lujano J, et al. Multi-objective optimization minimizing cost and life cycle emissions of stand-alone PV–wind–diesel systems with batteries storage. Appl Energy 2011;88:4033–41. http://dx.doi.org/10.1016/J.APENERGY.2011.04.019.

[15] Darling RM. Techno-economic analyses of several redox flow batteries using levelized cost of energy storage. Curr Opin Chem Eng 2022;37:100855. http://dx.doi.org/10.1016/J.COCHE.2022.100855.

[16] Sadeghi D, Ahmadi SE, Amiri N, Satinder, Marzband M, Abusorrah A, et al. Designing, optimizing and comparing distributed generation technologies as a substitute system for reducing life cycle costs, CO2 emissions, and power losses in residential buildings. Energy 2022;253:123947. http://dx.doi.org/10.1016/J.ENERGY.2022.123947.

[17] Shafik MB, Rashed GI, Chen H. Optimizing energy savings and operation of active distribution networks utilizing hybrid energy resources and soft open points: Case study in Sohag, Egypt. IEEE Access 2020;8:28704–17. http://dx.doi.org/10.1109/ACCESS.2020.2966909.

[18] Ardiles-Morales P, Zarate-Perez E, Cornejo-Carbajal C. Photovoltaic solar powered pumping system for agriculture in remote places. In: Proc LACCEI int multi-conference eng educ technol 2022. 2022, http://dx.doi.org/10.18687/LACCEI2022.1.1.303.

[19] US Department of Energy. NSRDB: National solar radiation database. 2022.

[20] Sengupta M, Xie Y, Lopez A, Habte A, Maclaurin G, Shelby J. The national solar radiation data base (NSRDB). Renew Sustain Energy Rev 2018;89:51–60. http://dx.doi.org/10.1016/j.rser.2018.03.003.

[21] Atia R, Yamada N. Sizing and analysis of renewable energy and battery systems in residential microgrids. IEEE Trans Smart Grid 2016;7:1204–13. http://dx.doi.org/10.1109/TSG.2016.2519541.

[22] Bukar AL, Tan CW, Lau KY. Optimal sizing of an autonomous photovoltaic/wind/battery/diesel generator microgrid using grasshopper optimization algorithm. Sol Energy 2019;188:685–96. http://dx.doi.org/10.1016/j.solener.2019.06.050.

[23] Chen SX, Gooi HB, Wang MQ. Sizing of energy storage for microgrids. IEEE Trans Smart Grid 2012;3:142–51. http://dx.doi.org/10.1109/TSG.2011.2160745.

[24] Ramli MAM, Bouchekara HREH, Alghamdi AS. Optimal sizing of PV/wind/diesel hybrid microgrid system using multi-objective self-adaptive differential evolution algorithm. Renew Energy 2018;121:400–11. http://dx.doi.org/10.1016/J.RENENE.2018.01.058.

[25] Rehman S, Al-Abbadi NM. Wind shear coefficients and energy yield for Dhahran, Saudi Arabia. Renew Energy 2007;32:738–49. http://dx.doi.org/10.1016/J.RENENE.2006.03.014.

[26] Bañuelos-Ruedas F, Angeles-Camacho C, Rios-Marcuello S. Analysis and validation of the methodology used in the extrapolation of wind speed data at different heights. Renew Sustain Energy Rev 2010;14:2383–91. http://dx.doi.org/10.1016/J.RSER.2010.05.001.

[27] Zarate-Perez E, Rosales-Asensio E, González-Martínez A, de Simón-Martín M, Colmenar-Santos A. Battery energy storage performance in microgrids: A scientific mapping perspective. Energy Rep 2022;8:259–68. http://dx.doi.org/10.1016/J.EGYR.2022.06.116.

[28] R Core Team. R: A language and environment for statistical computing. In: R foundation for statistical computing. Vienna, Austria; 2018, n.d.

[29] López-González A, Domenech B, Gómez-Hernández D, Ferrer-Martí L. Renewable microgrid projects for autonomous small-scale electrification in andean countries. Renew Sustain Energy Rev 2017;79:1255–65. http://dx.doi.org/10.1016/J.RSER.2017.05.203.

[30] Olaszi BD, Ladanyi J. Comparison of different discharge strategies of grid-connected residential PV systems with energy storage in perspective of optimal battery energy storage system sizing. Renew Sustain Energy Rev 2017;75:710–8. http://dx.doi.org/10.1016/J.RSER.2016.11.046.

[31] Khan H, Nizami IF, Qaisar SM, Waqar A, Krichen M, Almaktoom AT. Analyzing optimal battery sizing in microgrids based on the feature selection and machine learning approaches. Energies 2022;15:7865. http://dx.doi.org/10.3390/EN15217865, 2022;15:7865.